HHS Public Access

Author manuscript

*J Comp Neurol*. Author manuscript; available in PMC 2022 June 01.

Published in final edited form as:

*J Comp Neurol*. 2021 June ; 529(8): 1779–1786. doi:10.1002/cne.25056.

# Evolutionary and homeostatic changes in morphology of visual dendrites of Mauthner cells in *Astyanax* blind cavefish

**Zainab Tanvir**[1], **Daihana Rivera**[1], **Kristen E. Severi**[1], **Gal Haspel**[1], **Daphne Soares**[1,*]

[1]Federated Department of Biological Sciences, New Jersey Institute of Technology, Newark NJ 07102

## Abstract

Mauthner cells are the largest neurons in the hindbrain of teleost fish and most amphibians. Each cell has two major dendrites thought to receive segregated streams of sensory input: the lateral dendrite receives mechanosensory input while the ventral dendrite receives visual input. These inputs, which mediate escape responses to sudden stimuli, may be modulated by the availability of sensory information to the animal. To understand the impact of the absence of visual information on the morphologies of Mauthner cells during developmental and evolutionary time scales, we examined the teleost *Astyanax mexicanus*. This species of tetra is found in two morphs: a seeing surface fish and a blind cavefish. We compared the structure of Mauthner cells in surface fish raised under daily light conditions, in surface fish raised in constant darkness, and in two independent lineages of cave populations. The length of ventral dendrites of Mauthner cells in dark-raised surface fish larvae were longer and more branched, while in both cave morphs the ventral dendrites were smaller or absent. The absence of visual input in surface fish with normal eye development leads to a homeostatic increase in dendrite size, whereas over evolution, the absence of light led to the loss of eyes and a reduction in dendrite size.

## Graphical Abstract

[*]Corresponding Author Daphne Soares, Biological Sciences, New Jersey Institute of Technology, 100 Summit Street, Newark, NJ 07102, USA, Tel: 973 596 6421, soares@njit.edu.

Author Contributions

ZT, DS, KS, and GH conceived the project. ZT, DS, and DR collected and analyzed the data. All the authors discussed the project throughout and wrote the paper.

Animal husbandry and experimentation were covered under the Rutgers University IACUC protocol #201702685. NJIT is under Rutgers Newark IACUC oversight.

Statement of Ethics

No humans were used in this study.

Disclosure Statement

The authors have no conflicts of interest to declare.

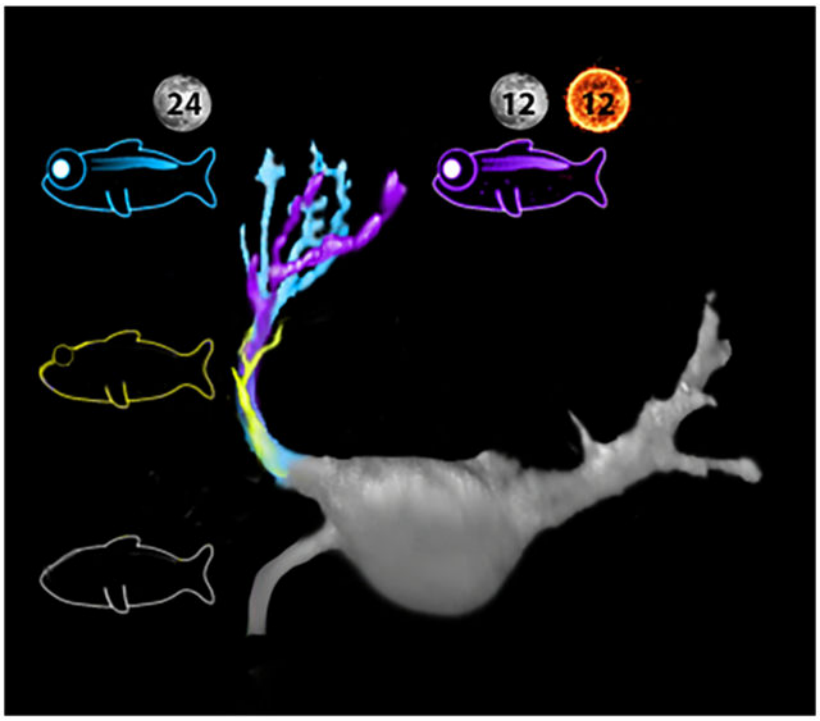


Development and Evolution influence the size and branching of visually targeted Mauthner cell dendrites.

**Keywords**

Evolution; neuron; fish; homeostasis; adaptation

## Introduction

Startle responses are rapid reactions that move an animal away from perceived danger (Peek and Card 2016). These behaviors are found in many species and are typically mediated by fast-acting neural circuits characterized by large diameter neurons and reduced numbers of synapses (Eaton and Hackett 1984; Eaton et al., 1988). Mauthner cells are a pair of large neurons found in the hindbrain of teleost fishes that mediate escape responses (Bartelmez 1915; Bullock 1978, 1984; Eaton et al., 2001). These neurons receive sensory input and project contralaterally descending axons onto primary motor neurons in the spinal cord (Kimmel et. al., 1981). Activation of a Mauthner cell results in rapid contraction of the contralateral musculature of the body trunk (Faber et al., 1989), leading to a stereotypical evasive maneuver known as a C-start (Eaton et al., 1991).

Each Mauthner cell has two large-diameter primary dendrites and each dendrite receives sensory information of different modalities. Acoustic and mechanosensory information targets the lateral dendrite (Zottoli, 1977; Eaton et al., 1988) while visual and somatosensory information is routed to the ventral dendrite (Faber and Korn, 1978; Zottoli et al., 1987, 1995; Canfield 2003). Visual inputs mediated by the ventral dendrite reliably produce rapid

escape responses across teleost species (Zottoli et. al 1987; Canfield 2006; Preuss et al., 2006; Dunn et al., 2016).

Troglobitic species throughout the world have convergent adaptations to life in caves, often including dramatic reductions of visual systems. Evolution in continual darkness has led to the degeneration of the visual system, and as animals become more cave-adapted, their eye structures are reduced and eventually vanish completely (Soares and Niemiller 2013; Barr, 1968; Fong et al., 1995; Protas and Jeffery, 2012; Culver and Pipan, 2015 ). The Mexican tetra fish, *Astyanax mexicanus* (Fig. 1), is extant in two morphs: an ancestral, river-dwelling morph (surface fish) and various derived, cave-dwelling morphs. Each lineage has unique adaptations to troglobitic life and is named after the cave in which they are endemic (Fig. 1a). There are two main lineages of fish that contain eyeless fish. The older lineage includes *Astyanax* cavefish from the Subterráneo, Pachón, and Chica populations (Dowling et al., 2002; Porter at al., 2007; Gross, 2012; Bradic et al., 2013). The younger lineage includes cavefish from the Los Sabinos, Curva, and Tinaja populations. These two lineages are morphologically distinct (Dowling et al., 2002; Fig. 1b).

Although adult *Astyanax* cavefish lack eyes, eye development is nevertheless initiated during embryogenesis (reviewed in Jeffery, 2001 and 2009; Krishnan et al., 2017; Emam et al., 2019). To examine the impact of the loss of visual input on neurons that mediate visually-triggered escape responses, we compared the morphologies of Mauthner cells in surface fish and in two lineages of cavefish. Interestingly, we found that the ventral dendrite that receives visual inputs was diminished or missing in both lineages of cavefish. To determine whether the loss of the ventral dendrite is caused by homeostatic mechanisms, we examined the morphologies of Mauthner cells of surface fish larvae raised in complete darkness. The ventral dendrites of dark-reared surface fish larvae are larger and more branched that of those reared under a daily light cycle. This result shows that in this case, evolutionary and homeostatic mechanisms operate in opposite directions.

## Materials and Methods

### Animal care

Fish larvae originated from a breeding colony and were kept at 20°C water temperature in either a 12h:12h light-dark cycle (12L:12D, surface fish) or constant darkness (24D, surface and cavefish). Breeding was induced by gradually increasing the water temperature from 20°C to 25°C over two days, and fertilized eggs were collected in meshed containers on the bottom of the tanks, based on the procedures of Dr. William Jeffery laboratory (University of Maryland). Animal husbandry and experimentation were covered under the Rutgers University IACUC protocol #201702685. NJIT is under Rutgers-Newark IACUC oversight.

### Retrograde labeling of Mauthner cells

We injected dye into Mauthner cell axons in larvae at 4 days post fertilization (dpf) by adapting previous protocols for backfilling reticulospinal neurons in teleosts (Fetcho and O'Malley, 1995; Orger et al., 2008). We used borosilicate capillary glass needles (thick-walled, with internal filaments, Cat 1B150F-4, VWR), pulled with a Flaming/Brown

micropipette puller (Model P-97, Sutter Instruments). We filled injection needles with 62.5 μg/μl of Dextran-TexasRed™, 3,000 molecular weight (Cat D3328, Invitrogen) or 20 μg/μl Dextran-Alexa488, 10,000 molecular weight (Cat D22910, Invitrogen). We broke the needle tips by gently swiping against the sharp open end of a Vannas-Tübingen Spring Scissor (Cat 15003-08, Fine Science Tools) to produce a jagged-edged opening.

Larvae were anaesthetized before injection in normal Ringer's solution (116 mM NaCl, 2.9 mM KCl, 1.8 mM CaCl2, 5.0 mM HEPES, pH 7.2; Westerfield, 2000) containing 0.3% ethyl 3-aminobenzoate methanesulfonate (Tricane; MS-222(Cat E10521, Sigma-Aldrich)). Anesthetized larvae were placed onto an agar-coated 35 mm Petri dish, and the injection needle was inserted laterally into the spinal cord with a micromanipulator (M3301R, Narishige International) under a dissecting light microscope (Olympus MVX10).

We injected caudal to the anal pore, approximately halfway between the anal pore and the end of the tail and took care to avoid injecting into blood vessels. To eject the dye from the pipette tip, we used a PicoPump (PV820, World Precision Instruments) with no more than 20 PSI of regulated house-air pressure. We let larvae recover in 24-well dishes in fresh fish water for at least 24 hours to allow for retrograde filling of reticulospinal cells. We screened larvae at 5 dpf, under an Olympus MVX10 stereoscope to confirm labeling of Mauthner cells before fixation.

## Fixation

We transferred 5 dpf larvae to 1.5 ml centrifuge tubes (Eppendorf). All fish water was aspirated and replaced with 1.0 ml 4% paraformaldehyde (Electron Microscopy Sciences, USA) in 1X PBS (Phosphate buffer saline, Fisher Scientific, USA). We fixed larvae overnight at 4°C and washed fixative three times with 1X PBS by aspirating and replacing PBS in a centrifuge tube. Fixed larvae can be stored for up to two weeks in 1X PBS.

## Image Acquisition

We dissected the brains of fixed larvae using custom-made tools made of sharpened tungsten wires attached to glass pipettes. We moved each brain to a drop of glycerol in a custom-made coverslip chamber. Briefly, we attached two 20×20 mm #1.5 coverslips to a 20×40 mm #1 coverslip with a room-temperature-hardening mixture made of equal weights of petroleum-jelly, lanolin, and paraffin (VALAP ), creating a vertical channel. We placed fixed brains in the channel, covered it with another 20×20 #1.5 coverslip and used VALAP to seal the channel. To image whole brains we used a laser scanning confocal microscope (Leica SP8; microscope: DM6000CS; objectives: Leica 20x/NA0.70 HC PL APO, Leica 40x/NA1.30 HC PL APO oil or Leica 63x/NA1.40 HC PL APO oil, with lateral resolutions of 414 nm, 223 nm, and 207 nm respectively; laser lines: 561 nm (for Dextran-TexasRed) and 488 nm (for Dextran-Alexa488)). We collected multiple optical slices (thickness optimized by the confocal software, ranging 0.34- 0.35 μm for the 63X objective, and 0.41- 0.42 μm for the 40X objective, and 0.95 μm for the 20X objective) that contained the complete dendritic structure of Mauthner cells in each brain.

### Image processing and Measurements

We processed images and measured features using a dedicated software package (Leica Application Suite X (LAS X) 3D Analysis module, Leica Microsystems). We used the viewer panel of the 3D Analysis module to linearly adjust the brightness and contrast of images of volume-rendered 3D objects. Next, we measured the maximum dendritic length from the edge of the soma to the farthest tip of VD with a line-measurement tool (adjusting the line to the dendrite from at least two orthogonal views), the maximum dendritic diameter, and the distance to the first branching point (i.e. length of the primary branch). We reduced background noise with a white noise reduction filter within the 3D Analysis module and cropped neighboring reticulospinal neurons labeled in the hindbrain with Adobe Illustrator to visually isolate the Mauthner cells. The branches of the ventral dendrite (VD) grow medially towards the soma at the terminus of the VD. We note that it is a hallmark of the VD in young Mauthner cells that finer neurites protrude laterally away from the soma and along the proximal length of the dendrite. We do not consider the finer neurites as branches for our analysis.

### Statistical Analysis

We compared experimental groups (Surface 24D, Tinaja and Pachón) to the control group (Surface 12L:12D) by estimation statistics that computes the effect size of each resample and determines 95% confidence intervals of the mean difference by performing 5,000 bootstrapping resamples (Ho et. al., 2019). We used ordered groups ANOVA test and two-sided permutation t-test to determine whether there were significant differences among the means of measurements. We considered an alpha value of 0.05 to be significant.

## Results

We examined Mauthner cells of *Astyanax mexicanus* larvae (Fig. 1) by retrograde labeling of the neurons with dextran-conjugated dyes, fixing and positioning the larvae to view the morphology of the labeled Mauthner cells located in the hindbrain (Fig. 2a inset). Mauthner cells have two primary dendrites: a lateral dendrite (LD) that receives auditory and lateral line input and a ventral dendrite (VD) that is thought to receive visual and tactile input (Medan et al., 2018). We compared the morphology of Mauthner cells of surface larvae raised under one of two conditions, a daily light cycle (12L:12D) or constant darkness (24D), and of cavefish of two lineages, to determine if morphological differences arise in the ventral dendrite if visual inputs were removed during development or evolution (Fig. 2). The maximum dendritic length to the farthest tip, number of dendritic tips, maximum dendritic diameter, and length of the primary dendrite of VDs in 24D surface fish larvae and in Pachón and Tinaja cavefish were significantly different from those in 12L:12D surface fish larvae (Fig. 3). The two cavefish lineages were also significantly different from each other in maximum dendritic length, number of dendritic tips, and maxiumum dendritic diameter.

VDs of 24D surface larvae were significantly longer (84.35±11.46 μm, $p<0.0001$), while VDs of Tinaja larvae were significantly shorter (22.44±19.62, $p=0.0028$) than 12D:12L surface larvae (54.76±8.67; Fig. 3a). Since Pachón cavefish larvae did not have VDs (Fig. 2d

and Fig. 4d1-d6), their length was recorded as 0 ($p<0.0001$ compared to 12L:12D surface fish and $p=0.009$ to Tinaja cavefish; Fig. 3a).

In 12L:12D surface larvae (Fig. 2a and Fig. 4a1-a6) VDs began with a 2.98±0.5 μm diameter primary branch with several finer processes protruding medially (Fig. 3c). The primary branch branched once after 32.86±7.83 μm into two terminal branches (Fig. 3b, d). In 24D surface larvae (Fig. 2b and Fig. 4b1-b5), VD primary branches were thicker and longer than controls (4.5±0.89 μm, $p=0.02198$; 43.09±9.95 μm, Fig. 3c, d). They often arborized into three or more terminal branches (Fig. 3b) and also displayed fine medial processes off the length of the dendrite. In Tinaja cavefish, the neurons appeared overall smaller than in surface fish (Fig. 2c and Fig. 4c1-c7) with occasional branching of VD (Fig. 3b) that appeared thin (diameter 1.73±1.36 μm; Fig. 3c) and truncated with fine medial processes. In the three Tinaja larvae in which the VD did branch, the primary branches were 19.78±5.07 μm long, shorter than the primary branches of 12L:12D surface larvae ($p<0.0001$).

The number of dendritic tips is a measure of terminal branching (Fig. 3b). VDs of 24D surface larvae were more arborized than the stereotypic bifurcated VD of 12L:12D surface larvae ($p=0.0008$), while VDs of Tinaja larvae were less arborized ($p=0.0082$). Since Pachón cavefish larvae did not have VDs, their numbers of dendritic tips were recorded as 0 ($p<0.0001$ to control-raised surface fish; Fig. 3b).

Furthermore, we measured the total length and thickness of lateral dendrites from each of the four groups. The lengths of lateral dendrites of the four groups were not significantly different from each other: 37.37±11.08 μm for 12L:12D surface larvae, 50.35±15.28 μm for 24D surface larvae, 30.42±10.71 μm for Tinaja larvae, and 41.67±12.52 μm Pachón larvae (Fig. 5a). In contrast, the lateral dendrites of 12L:12D surface larvae were thinner than those of 24D surface larvae (6.00±1.12 μm and 8.07±0.98 μm, respectively; $p=0.022$), and thicker than those of Pachón (4.43±0.88 μm; $p=0.0132$), but not different than the lateral dendrites of Tinaja larvae (5.48±1.47 μm)(Fig. 5b).

## Discussion

One of the most intriguing questions in Biology is how evolution changes phenotypes and how evolutionary pressure interacts with homeostatic changes that occur on a much shorter time scale. Do homeostatic responses provide a mechanism for evolutionary modifications? Or conversely, are evolutionary modifications the outcomes of generations of unbalanced homeostatic responses? The latter seems to be a simple and straightforward explanation of how adaptation could be influenced by homeostatic mechanisms. However, here we have found at least one example of a homeostatic response that leads to the opposite outcome than an evolutionary adaptation.

To examine the influence of the visual environment on the developing circuit, we raised surface morph larvae of *Astyanax mexicanus* in constant darkness. We predicted that in these fish the ventral dendrite would be smaller, but instead, the dendrite was not only longer, but also much more branched than daily light (control) raised fish. This is interesting because it is consistent with the work of Shtanchaev et al. (2008), where they showed

morphological plasticity of the ventral dendrite of the Mauthner cell in the goldfish depending on the level of stimulation. In those fish there is a negative correlation between size and level of stimulation. We have shown that *Astyanax mexicanus* surface fish display the commonly found Mauthner cell morphology, which is shared among fishes and amphibians. However, the cavefish morphs have either much smaller or absent ventral dendrites, depending on the duration of the cavefish lineage isolation in the darkness of a cave.

*Astyanax* as a model animal allowed us to study two different time scales for changes in the morphology of a dendrite involved in visually-guided behavior: early development and evolution. Conceptually, homeostatic mechanisms hinder changes, whereas evolutionary processes drive them. Here, the evolutionary changes in larval *Astyanax* were caused by adaptation to troglobitic life, including the loss of eyes and concomitant changes in neural control networks that rely on vision. Homeostatic regulation was caused by rearing surface fish in complete darkness, eliminating visual signals during development. We compared each of these groups to the basal morphology exhibited by surface fish raised in alternating light and dark epochs like those that the fish experience in nature.

We expected both time scales to follow the same path, and our main findings show that cave adaptation is correlated with a decrease the size of the dendrite in an evolutionary time scale of tens of thousands of years, but during development occurring over days, darkness has the opposite effect, increasing the size and complexity of the visual dendrite. A possible outcome would have been that cavefish maintained their visual dendrites after cave adaptation, and these dendrites were co-opted by another sensory modality. Another reasonable outcome would have been that dark reared surface fish lost, or at least decreased, visual dendrites. We found neither of these outcomes in *Astyanax*. Instead, reduced input during the time scale of development resulted in an increase in the morphological complexity of ventral dendrites, an opposite result from the evolutionary time scale.

It has been a long-standing question why in rivers with so many species of teleosts, only *Astyanax* has been the one to colonize caves successfully, and multiple times (Bilandžija et al., 2020; Yoffe et al. 2020). Here, we added neuromorphological homeostasis to the body of evidence that argues for *Astyanax* as a particularly plastic species, which is advantageous for dispersal. Accordingly, homeostatic mechanisms are under natural selection, providing malleability for adaptation to constant darkness.

## Acknowledgement

We would like to thank Marina Yoffe for the collection of *Astyanax* eggs and Dr. Eric Fortune for their helpful comments on the manuscript. We thank Kathryn Gallman for the fish care.

Funding Sources

Grant support: NIH R15EY027112.

The data that support the findings of this study are available from the corresponding author upon reasonable request.

## References


Barr TC (1968). Cave ecology and the evolution of troglobites. In Evolutionary biology (pp. 35–102). Springer, Boston, MA.

Bartelmez GW (1915) Mauthner's cell and the nucleus motorius tegmenti. Journal of Comparative Neurology. 25(1):87–128.

Bilandžija H, Hollifield B, Steck M, Meng G, Ng M, Koch AD, Gračan R, Ćetković H, Porter ML, Renner KJ, Jeffery WR (2020) Phenotypic plasticity as a mechanism of cave colonization and adaptation. Elife. 9:e51830. [PubMed: 32314737]

Bradic M, Teotónio H, & Borowsky RL (2013). The population genomics of repeated evolution in the blind cavefish Astyanax mexicanus. Molecular biology and evolution, 30(11), 2383–2400. [PubMed: 23927992]

Bullock TH (1978) Indetifiable and addressed neurons in the vertebrates. In Neurobiology of the Mauthner cell. Eds. Faber D and Kom H, Raven press, New York, 1–12.

Bullock TH (1984) Comparative neuroethology of startle, rapid escape, and giant fiber-mediated responses. In Neural Mechanisms of Startle Behavior. Ed Eaton RC, Plenum press, New York. 1–13.

Canfield JG (2003) Temporal constraints on visually directed C-start responses: behavioral and physiological correlates. Brain, behavior and evolution. 61(3):148–58.

Canfield JG (2006) Functional evidence for visuospatial coding in the Mauthner neuron. Brain, behavior and evolution. 67(4):188–202.

Culver D, Pipan T (2015). Shifting paradigms of the evolution of cave life. Acta Carsologica, 44(3).

Dowling TE, Martasian DP, Jeffery WR (2002) Evidence for multiple genetic forms with similar eyeless phenotypes in the blind cavefish, Astyanax mexicanus. Molecular biology and evolution. 19(4):446–55. [PubMed: 11919286]

Dunn TW, Gebhardt C, Naumann EA, Riegler C, Ahrens MB, Engert F, Del Bene F (2016) Neural circuits underlying visually evoked escapes in larval zebrafish. Neuron. 89(3):613–28. [PubMed: 26804997]

Eaton RC, Hackett JT (1984) The role of the Mauthner cell in fast-starts involving escape in teleost fishes. In Neural mechanisms of startle behavior (pp. 213–266). Springer, Boston, MA.

Eaton RC, DiDomenico R, Nissanov J (1988) Flexible body dynamics of the goldfish C-start: implications for reticulospinal command mechanisms. Journal of Neuroscience. 8(8):2758–68. [PubMed: 3411353]

Eaton RC, Emberley DS (1991) How stimulus direction determines the trajectory of the Mauthner-initiated escape response in ateleost fish. Journal of Experimental Biology. 161(1):469–87.

Eaton RC, Lee RK, Foreman MB (2001) The Mauthner cell and other identified neurons of the brainstem escape network of fish. Progress in neurobiology. 63(4):467–85. [PubMed: 11163687]

Emam A, Yoffe M, Cardona H, Soares D (2020). Retinal morphology in *Astyanax mexicanus* during eye degeneration. Journal of Comparative Neurology, 528(9):1523–1534.

Faber DS, Korn H., editors. (1978) Neurobiology of the Mauthner cell. Raven Press.

Faber DS, Fetcho JR, Korn H (1989) Neuronal Networks Underlying the Escape Response in Goldfish: General Implications for Motor Control a. Annals of the New York Academy of Sciences. 563(1):11–33. [PubMed: 2672948]

Fetcho JR, O'Malley DM (1995) Visualization of active neural circuitry in the spinal cord of intact zebrafish. Journal of neurophysiology, 73(1), pp.399–406. [PubMed: 7714582]

Fong DW, Kane TC, Culver DC (1995). Vestigialization and loss of nonfunctional characters. Annual Review of Ecology and Systematics, 26(1), 249–268.

Gross JB (2012). The complex origin of *Astyanax* cavefish. BMC evolutionary biology, 12(1), 105. [PubMed: 22747496]

Ho J, Tumkaya T, Aryal S, Choi H, Claridge-Chang A (2019). Moving beyond P values: data analysis with estimation graphics. Nature methods, 16(7), 565–566. [PubMed: 31217592]

Jeffery WR (2001). Cavefish as a model system in evolutionary developmental biology. Developmental biology, 231(1), 1–12. [PubMed: 11180948]

Jeffery WR (2009). Regressive evolution in *Astyanax* cavefish. Annual review of genetics, 43, 25–47.

Kimmel CB, Sessions SK, Kimmel RJ (1981). Morphogenesis and synaptogenesis of the zebrafish Mauthner neuron. Journal of Comparative Neurology, 198(1), 101–120.

Krishnan J, Rohner N (2017). Cavefish and the basis for eye loss. Philosophical Transactions of the Royal Society B: Biological Sciences, 372(1713), 20150487.

Medan V, Maki-Märttunen T, Sztarker J, Preuss T. (2018) Differential processing in modality-specific Mauthner cell dendrites. The Journal of physiology. 596(4):667–89. [PubMed: 29148564]

Orger MB, Kampff AR, Severi KE, Bollmann JH, Engert F (2008) Control of visually guided behavior by distinct populations of spinal projection neurons. Nature neuroscience, 11(3), pp.327–333. [PubMed: 18264094]

Peek MY, Card GM (2016). Comparative approaches to escape. Current Opinion in Neurobiology, 41, 167–173. [PubMed: 27710794]

Porter ML, Dittmar K, Pérez-Losada M (2007). How long does evolution of the troglomorphic form take? Estimating divergence times in Astyanax mexicanus. Acta carsologica, 36(1).

Preuss T, Osei-Bonsu PE, Weiss SA, Wang C, Faber DS (2006) Neural representation of object approach in a decision-making motor circuit. Journal of Neuroscience. 2006 3 29;26(13):3454–64. [PubMed: 16571752]

Protas M, Jeffery WR (2012). Evolution and development in cave animals: from fish to crustaceans. Wiley Interdisciplinary Reviews: Developmental Biology, 1(6), 823–845. [PubMed: 23580903]

Shtanchaev RS, Mikhailova GZ, Dektyareva NY, Kokanova NA, Moshkov DA (2008). Changes in the ventral dendrite of Mauthner neurons in goldfish after optokinetic stimulation. Neuroscience and behavioral physiology, 38(9), 917–921. [PubMed: 18975109]

Soares D and Niemiller ML, (2013) Sensory adaptations of fishes to subterranean environments. BioScience, 63(4), pp.274–283.

Westerfield M (2000). The zebrafish book. A guide for the laboratory use of zebrafish (Danio rerio). 4th ed., Univ. of Oregon Press, Eugene.

Yoffe M, Patel K, Palia E, Kolawole S, Streets A, Haspel G Soares D (2020). Morphological malleability of the lateral line allows for surface fish (*Astyanax mexicanus*) adaptation to cave environments. Journal of Experimental Zoology Part B: Molecular and Developmental Evolution.

Zottoli SJ (1977). Correlation of the startle reflex and M cell auditory responses in unrestrained goldfish. J. Exp. Biol 66, 243–254. [PubMed: 858992]

Zottoli SJ, Hordes AR, Faber DS (1987) Localization of optic tectal input to the ventral dendrite of the goldfish Mauthner cell. Brain research. 401(1):113–21. [PubMed: 3815088]

Zottoli SJ, Bentley AP, Prendergast BJ, Rieff HI (1995) Comparative studies on the Mauthner cell of teleost fish in relation to sensory input. Brain, behavior and evolution. 46(3):151–64.

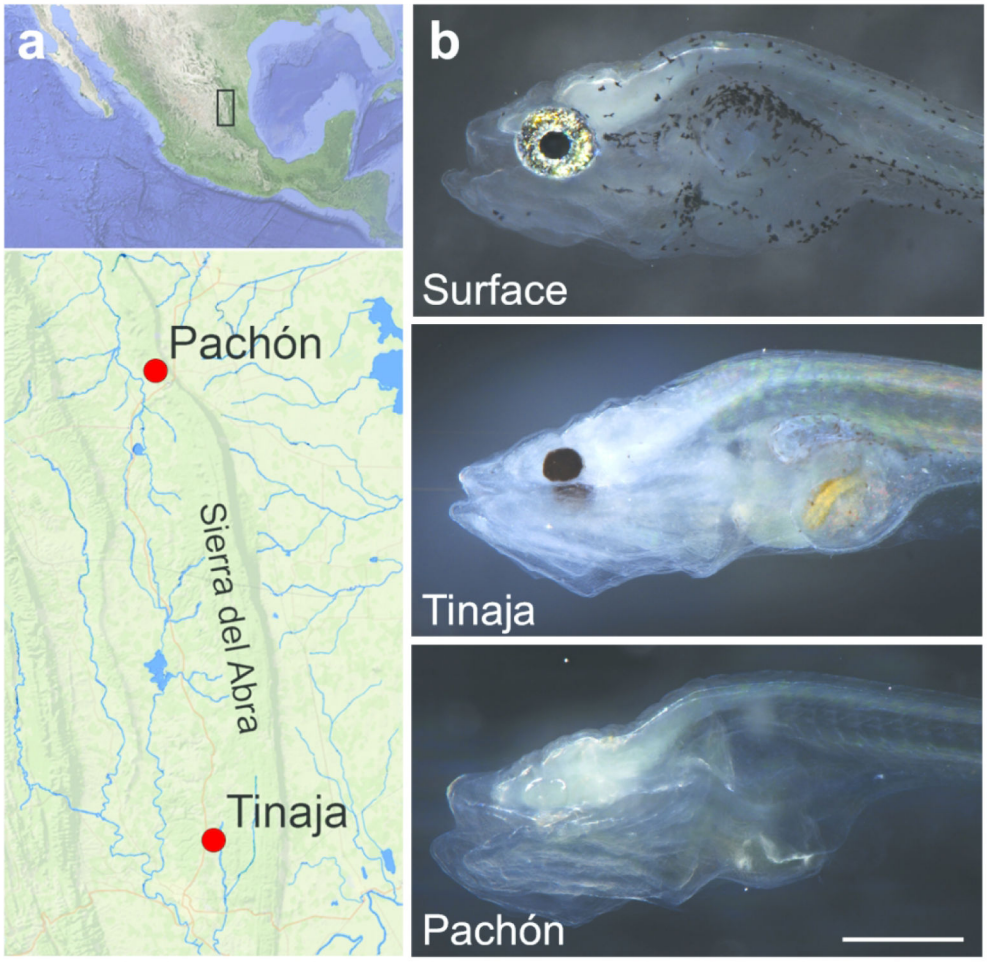


**Figure 1:**

Distribution and morphology of Astyanax mexicanus morphs used in this study. (a) Tinaja and Pachón morphs are geographically isolated in caves with these names in the Sierra del Abra region of Mexico (Tinaja: 22°04’34”N 98°58’40”W; Pachón: 22°36’25”N 99°02’55”W). Blue lines represent rivers in the area inhabited by the surface morph. Images from Google Earth. (b) Surface fish have pigmented eyes and skin, whereas Tinaja cavefish only have pigmented pupils and Pachón cavefish have no pigment on their skin or eyes. 7 dpf larvae. Common scale bar: a. 10 km b. 0.5 mm.

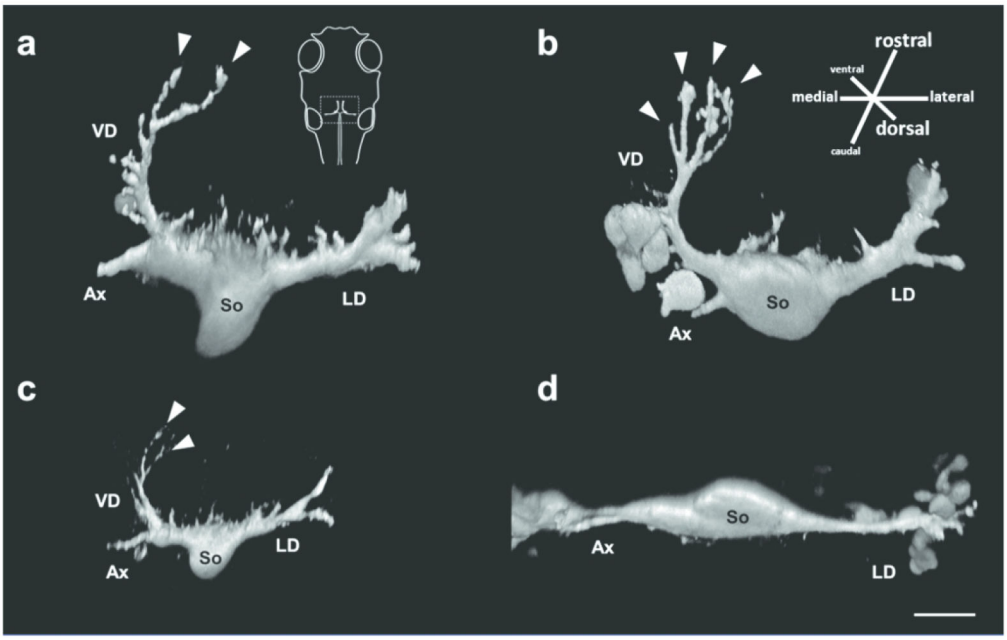


**Figure 2:**

Neuronal morphology differs among Mauthner cells in surface fish raised in different light conditions, and in Tinaja and Pachón cavefish. Volume rendering of representative right Mauthner cells of (a) surface fish raised in 12L:12D conditions, note the ventral dendrite (VD) and two dendritic tips; (b) Mauthner cell of surface fish raised in 24D conditions, note four dendritic tips on the ventral dendrite. (c) Mauthner cell of Tinaja cavefish, note the ventral dendrite is smaller than those of surface fish. (d) Mauthner cell of Pachón cavefish, note the absence of ventral dendrite. VD: ventral dendrite, LD: lateral dendrite, So: soma, Ax: axon, arrowheads: dendritic tips. All neurons from 5 dpf larvae. Scale bar: 20 μm.

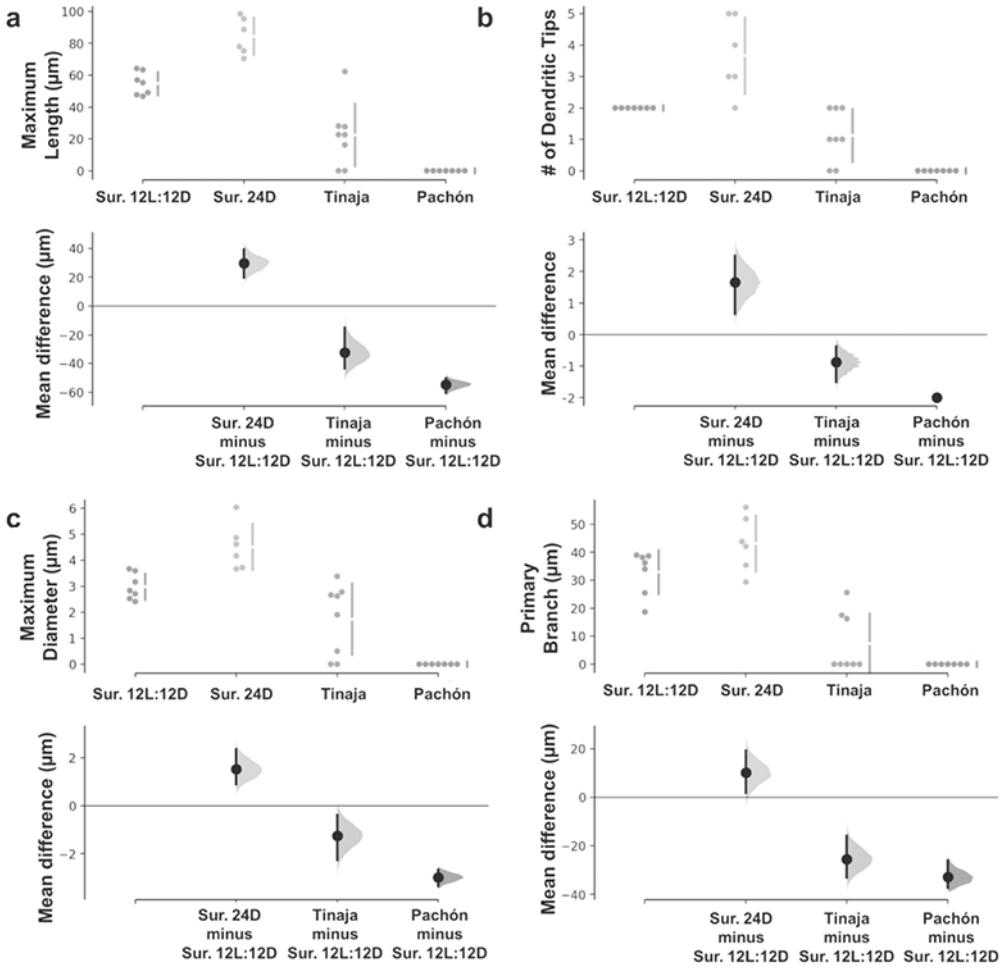


**Figure 3:**

Mauthner cell ventral dendrites of surface fish increase in length and number of branches when raised in 24D conditions, while cavefish dendrites are smaller or absent. (a) Maximum dendritic length. (b) Number of dendritic tips. (c) Maximum dendritic diameter. (d) Length of primary branch. Three comparisons against the shared control surface (Sur.) 12L:12D are shown in Cumming estimation plots in which the raw data is plotted on the upper axes. On the lower axes, mean differences are plotted as bootstrap sampling distributions, each mean difference is depicted as a dot, and each 95% confidence interval is indicated by the ends of the vertical error bars. The numbers of neurons (animals) are Surface (Sur.) 12L:12D: n= 7 (5), Surface (Sur.) 24D: n= 6 (3), Tinaja: n= 8 (5), Pachón: n= 7 (4).

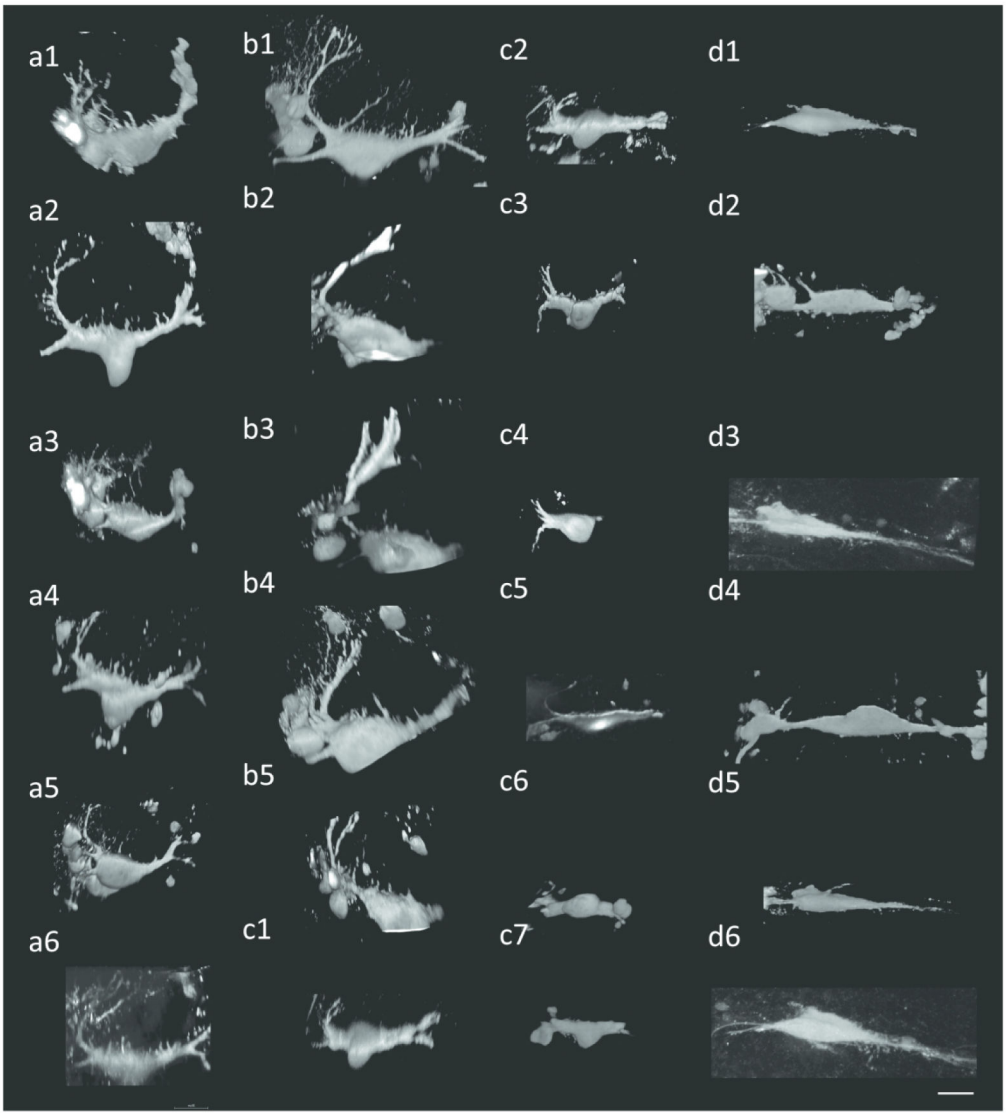


**Figure 4:**
Mauthner cell morphology is variable among morphs and experimental conditions. (a1-a6) Surface 12L:12D (b1-b5) Surface 24D (c1-c7) Tinaja (d1-d6) Pachón. Scale bar: 20 μm.

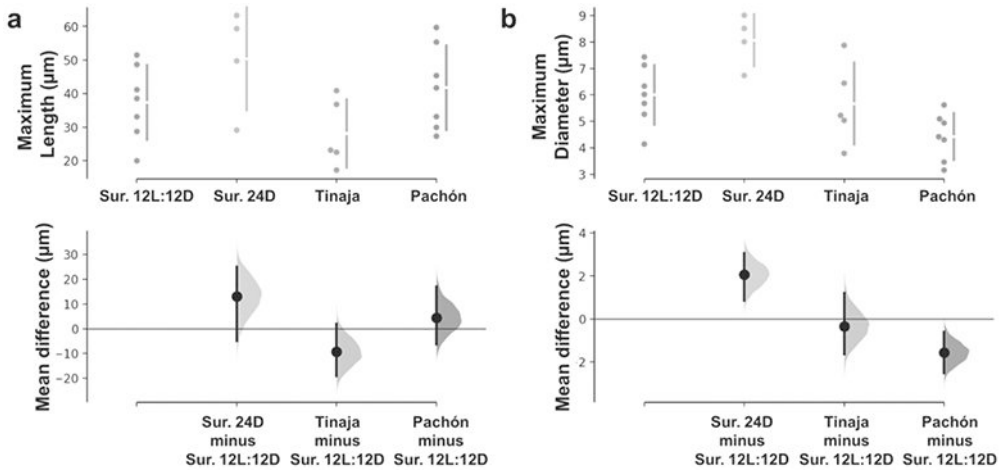


**Figure 5:**

Lateral dendrites are similar in length among all groups, but LD of surface fish larvae raised in 12L:12D are thinner than those of larvae raised in 24D and thicker than those of Pachón. (a) Maximum length of lateral dendrites. (b) Maximum diameter of lateral dendrites. Three comparisons against the shared control Surface (Sur.) 12L:12D are shown in Cumming estimation plots in which the raw data is plotted on the upper axes. On the lower axes, mean differences are plotted as bootstrap sampling distributions, each mean difference is depicted as a dot, and each 95% confidence interval is indicated by the ends of the vertical error bars. The numbers of neurons (animals) are Surface (Sur.) 12L:12D: n= 7 (5), Surface (Sur.) 24D: n= 4 (2), Tinaja: n= 6 (4), Pachón: n= 7 (4).